A. Yücel Odabaşı Colloquium Series
5th International Meeting on Advances in Marine Robotics and Autonomous Systems
18th–19th December 2025, Istanbul, Turkey

Curvature-Based Vessel Motion Modeling: A Kinematic Approach for Path Planning and Predictive

Ferhan Büyükçolak[1*], Gökhan Tansel Tayyar[2]

[1] *University of Genoa, DITEN, 16126 Via Balbi 5, Genoa Italy*
[2] *Istanbul Technical University, Faculty of Naval Architecture and Ocean Engineering, 34469 Maslak Istanbul Turkey*

Abstract: This paper presents a novel curvature-based kinematic framework for unmanned surface vessel (USV) path planning that directly incorporates vessel maneuvering constraints into the planning process. The proposed method reformulates the classical kinematic model using curvilinear coordinates parameterized by curvature κ and arc length s, enabling natural enforcement of minimum turning radius constraints while maintaining computational efficiency. A hierarchical planning architecture is developed, combining quadtree-based visibility graphs for global collision-free path generation with nonlinear model predictive control (NMPC) for trajectory refinement. The curvilinear formulation employs a sinc-based discretization that eliminates numerical discontinuities between straight and curved segments, ensuring smooth control profiles throughout the paths. Simulation results demonstrate effective navigation in complex multi-obstacle environments, with the method rapidly producing feasible trajectories that respect the speed-varying geometric constraints inherent to vessel maneuvering. The steady-state assumption employed provides robustness to model uncertainties while maintaining paths feasibility. This work advances autonomous maritime navigation by bridging the gap between geometric path planning and vessel dynamics, offering a practically implementable solution that ensures both computational efficiency and dynamic feasibility.
Keywords: Path planning, Nonlinear model predictive control, Arc-length parameterization, paths smoothing, Maritime navigation

1 INTRODUCTION

Path planning for unmanned surface vessels (USVs) must account for physical constraints beyond collision avoidance and path length minimisation. Unlike ground robots that can execute sharp waypoint transitions, USVs must satisfy strict curvature and smoothness constraints due to hydrodynamic characteristics. The minimum turning radius increases with surge speed and is limited by the maximum rudder deflection, making high speed tight turns physically impossible without deceleration (Belleter et al., 2016; Abrougui et al., 2021). This fundamental limitation renders traditional waypoint chains of straight segments unsuitable for many marine applications. The difficulty is acute in confined or obstacle dense waterways where global planners often produce shortest paths without considering speed dependent manoeuvring limits. Feasibility is then delegated to the tracking controller, creating curvature discontinuities at waypoint junctions and turns that exceed the vessel's capability at the planned speed. The mismatch between geometrically optimal paths and dynamically feasible trajectories leads to tracking errors, excessive control effort, or forced speed reductions that compromise mission efficiency. Curvature aware planning has therefore become essential for autonomous marine navigation. Approaches include continuous curvature primitives such as clothoids, Bézier curves, and splines (Scheuer and Fraichard, 1997; Xu et al., 2021; Hassani and Lande, 2018), as well as optimisation frameworks that minimise curvature or curvature variation (Heilmeier et al., 2020; Rao et al., 2024; Candeloro et al., 2013). Related work addresses multi agent coordination under curvature limits (Lobaton et al., 2011; Song et al., 2024; Tam and Bucknall, 2010) and environmental adaptation for terrain or surface following (Cui et al., 2022; Sinha et al., 2025). However, many methods either rely on complex dynamic models with high computational cost or use simplified kinematics that insufficiently capture manoeuvring constraints. We bridge this gap by reformulating vessel kinematics in curvilinear coordinates parameterised by curvature κ and arc length s. This representation maps naturally to control inputs: under steady state calibration, curvature is monotonically related to rudder angle, and arc length increment relates directly to surge speed. In this frame, speed dependent turning limits enter as simple curvature bounds, $|\kappa(s)| \leq 1/R_{\min}(u)$, where $R_{\min}(u)$ is the minimum turning radius at speed u. Our planning pipeline combines a quadtree based visibility graph for global, collision free routing with an offline nonlinear model predictive refinement that enforces curvature continuity and respects manoeuvring limits derived from steady state turning data. A key numerical ingredient is a sinc based discretisation that unifies straight and curved motion, removing the singular behaviour as curvature tends to zero and ensuring smooth transitions along the path. The

** Corresponding author e-mail: ferhan.buyukcolak@edu.unige.it

approach remains computationally efficient at the planning stage while preserving geometric exactness. The contributions are threefold: (i) a curvilinear kinematic formulation that enables closed form reconstruction from curvature profiles to Cartesian paths, (ii) a numerically robust discretisation that yields a single continuous update for zero and nonzero curvature, and (iii) a hierarchical architecture that separates global collision avoidance from local feasibility refinement. Simulations in multi obstacle environments produce smooth trajectories that respect speed varying geometric constraints while maintaining computational tractability.

The remainder of this paper is structured as follows. Section 2 introduces the proposed methodology, beginning with a discussion of curvature-constrained planning, followed by the derivation of the curvilinear kinematic formulation, the sinc-based discretization scheme, and the hierarchical planning pipeline integrating global visibility-graph path generation with offline NMPC refinement. Section 3 presents numerical results and discusses the effectiveness of the proposed approach through multiple simulation scenarios, highlighting the impact of curvature limits and obstacle configurations on paths smoothing. Finally, Section 4 concludes the paper by summarizing the main contributions, discussing practical implications, and outlining directions for future work.

2 METHODOLOGY

2.1 Background on curvature-constrained planning

Every nonholonomic platform has a finite turning radius; enforcing curvature bounds improves feasibility, safety, energy use, and tracking authority. In practice, a hard bound on curvature keeps trajectories within the minimum turning radius, limits heel and skidding, reduces rudder activity, and prevents actuator saturation (Ravankar et al., 2018; Mac et al., 2016). To obtain smooth, controller-friendly references, planners either use continuous-curvature primitives (clothoids, Bézier curves, splines) (Scheuer and Fraichard, 1997; Xu et al., 2021; Hassani and Lande, 2018) or optimise curvature and its variation directly (Heilmeier et al., 2020; Rao et al., 2024; Candeloro et al., 2013). Our approach embeds these limits kinematically via a curvilinear formulation and refines collision-free routes into dynamically feasible references.

2.2 Steady-state curvature map

At a given propeller setting (rpm), a commanded rudder angle δ produces steady circular motion with turning radius $R(\delta, \mathrm{rpm})$ obtained from standard turning-circle trials. The steady curvature is

$$\kappa_{ss}(\delta, \mathrm{rpm}) = \frac{1}{R(\delta, \mathrm{rpm})}. \tag{1}$$

Because $R(\delta, \mathrm{rpm})$ is measured on steady trajectories, in-turn speed loss and rudder-induced drag are implicitly included; no explicit yaw-rate or drag model is required for geometry. Feasible paths then satisfy a speed-dependent bound

$$|\kappa(s)| \le \kappa_{\max}(u) := \frac{1}{R_{\min}(u)}. \tag{2}$$

Speed affects only timing, not geometry: with $\mathrm{d}s = U(t)\,\mathrm{d}t$,

$$t(s) = \int_0^s \frac{1}{U(\sigma)}\,\mathrm{d}\sigma, \tag{3}$$

where the curve traced by $\kappa(s)$ in (x, y) is invariant to $U(t)$.

2.3 Curvilinear kinematics in arc length

Let s denote arc length and χ the course (tangent) angle. The particle-kinematic model is

$$\frac{\mathrm{d}x}{\mathrm{d}s} = \cos\chi(s), \qquad \frac{\mathrm{d}y}{\mathrm{d}s} = \sin\chi(s), \qquad \frac{\mathrm{d}\chi}{\mathrm{d}s} = \kappa(s). \tag{4}$$

For a rigid hull, heading ψ and sideslip β satisfy $\chi = \psi + \beta$. Under steady-state calibration, κ is monotonically related to the rudder angle δ, and $\mathrm{d}s$ relates directly to surge speed, making (4) a compact vehicle-agnostic description for planning.

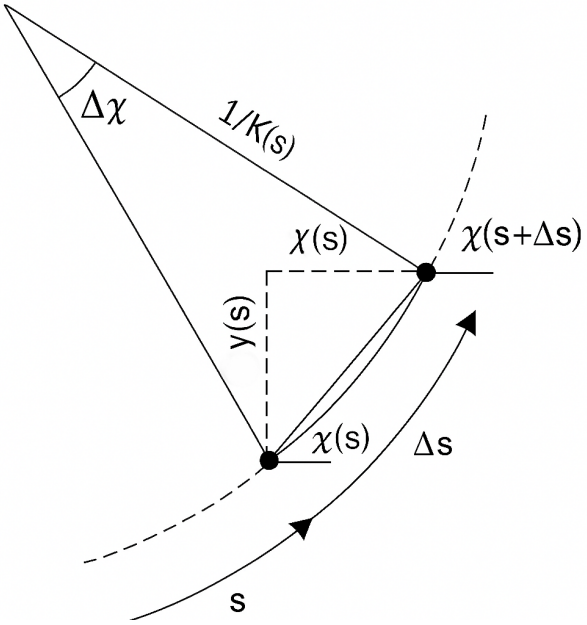

Figure 1: Curvilinear coordinates

Figure 2 illustrates the trajectories generated for different curvature values κ. Each colored curve corresponds to a constant curvature level, ranging from negative to positive values, which represent left- and right-turning motions, respectively. The figure clearly shows how increasing the magnitude of κ leads to tighter paths bending, whereas values close to zero result in nearly straight paths. Since curvature κ is directly related to the vehicle's velocity, this visualization demonstrates not only the effect of curvature on the geometric shape of the paths but also highlights how paths smoothing inherently accounts for the vehicle's dynamic motion characteristics that vary with speed.

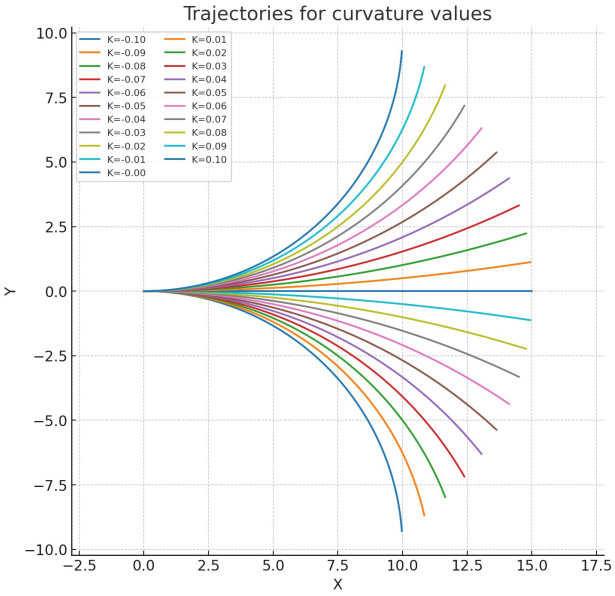

Figure 2: Trajectories generated for different curvature values κ, illustrating the effect of curvature magnitude on paths bending.

2.4 Sinc discretisation: unified and numerically robust update

Discretise the path with step Δs and assume piecewise-constant curvature κ_k over $[s_k, s_{k+1}]$. Let $\Delta\chi = \kappa_k \Delta s$. Then

$$\chi_{k+1} = \chi_k + \Delta\chi. \tag{5}$$

Starting from

$$\Delta x = \int_{s_k}^{s_{k+1}} \cos\chi(\sigma)\,\mathrm{d}\sigma = \int_{\chi_k}^{\chi_{k+1}} \frac{\cos\chi}{\kappa_k}\,\mathrm{d}\chi, \tag{6}$$

$$\Delta y = \int_{s_k}^{s_{k+1}} \sin\chi(\sigma)\,\mathrm{d}\sigma = \int_{\chi_k}^{\chi_{k+1}} \frac{\sin\chi}{\kappa_k}\,\mathrm{d}\chi, \tag{7}$$

substitute $\kappa_k = \Delta\chi/\Delta s$ and apply the sum/difference half-angle identities. One obtains the unified updates

$$x_{k+1} = x_k + \Delta s\ \mathrm{sinc}\Big(\tfrac{\Delta\chi}{2}\Big)\ \cos\Big(\chi_k + \tfrac{\Delta\chi}{2}\Big), \tag{8}$$

$$y_{k+1} = y_k + \Delta s\ \mathrm{sinc}\Big(\tfrac{\Delta\chi}{2}\Big)\ \sin\Big(\chi_k + \tfrac{\Delta\chi}{2}\Big), \tag{9}$$

with $\mathrm{sinc}(x) = \sin x/x$ and $\mathrm{sinc}(0) = 1$. These expressions are continuous as $\Delta\chi \to 0$ and reduce exactly to straight-line motion when $\kappa_k = 0$. Under the piecewise-constant curvature assumption the scheme is exact for constant curvature and, via a midpoint interpretation, second-order accurate for slowly varying curvature.

2.5 Planning pipeline: visibility-graph global path and offline refinement

Global path. We build a visibility graph augmented with quadtree sampling of free-space cell centres. Nodes comprise the start n_I, goal n_G, buffered obstacle vertices, and selected quadtree centres; edges connect line-of-sight pairs within free space and are weighted by Euclidean distance. A* search yields a collision-free, near-shortest waypoint chain (LOZANO-PÉREZ,Weslet,A., 1979; Samet, Hanan, and Robert E. Webber., 1985; Hart, Peter E. and Nilsson, Nils J. and Raphael, Bertram., 1968; Shah, 2016).

Offline refinement (NMPC over curvilinear states). Given the waypoint chain, we optimise over $\{\kappa_k, \Delta s_k\}_{k=0}^{N-1}$ with state (x_k, y_k, χ_k) and dynamics (5)–(9). Constraints include curvature limits $|\kappa_k| \le \kappa_{\max}(u_k) = 1/R_{\min}(u_k)$ from the steady-state map $\kappa_{ss}(\delta, \mathrm{rpm})$, $\Delta s_k \ge 0$, and obstacle clearance consistent with the global buffer. A typical stage cost is

$$\ell_k = w_p \|[x_k, y_k] - [x_k^{\mathrm{ref}}, y_k^{\mathrm{ref}}]\|_2^2 + w_\kappa(\kappa_k - \kappa_{k-1})^2 + w_s(\Delta s_k - \bar{s})^2,$$

solved offline in CasADi/IPOPT. The output $\{x_k, y_k, \chi_k, \kappa_k, \Delta s_k\}$ removes curvature discontinuities at waypoint junctions and respects the minimum turning radius at the planned operating speed.

2.6 Identification, validation, and practical notes

Turning-circle trials across several δ and rpm settings provide R_{ss} and in-turn speed U_{turn}; we set $\kappa_{ss} = 1/R_{ss}$ and fit a smooth surface $\kappa(\delta, \mathrm{rpm})$ (e.g., splines) with correct $\partial\kappa/\partial\delta$ sign. Validation compares refined paths to independent manoeuvres (zigzag, Williamson) and reports feasibility (no bound violations), path-length overhead, and solver time. Disturbances (wind, waves, currents), shallow-water effects, and loading changes may shift effective curvature; these can be handled via feedback during tracking or by extending the curvature map to condition-dependent bounds. The steady-state assumption neglects transients, making the refined paths conservative in emergencies while highly efficient for planning.

3 NUMERICAL RESULTS AND DISCUSSION

This section first presents the methodology employed to adapt linearly generated path segments between waypoints to the dynamic constraints of the vehicle. Subsequently, the text provides a detailed exposition of the refinement of paths obtained through a quadtree-based visibility graph in environments with convex obstacles using an optimization-based smoothing approach. The configurations of the NMPC solver used in the optimization process for smoothing are spread over a solution horizon of 25 steps. The number of iterations in each step is 500 when IPOPT is used as the solver. In the first three scenarios, one of the terms representing the vehicle's physical constraints, ds, is set to 5. The value of K, representing the vehicle's speed-dependent turning radius, is set to 0.1 in the first scenario. In scenarios two and three, it is set to 0.01 and 0.03, respectively, to demonstrate the effect of turning radii on path smoothing. All scenario optimizations were carried out using the CasADi optimization toolbox, executed on an Intel® Core™ i7-11800H processor (24M Cache, 2.30 GHz, up to 4.60 GHz). For an MPC setup with a 25-step prediction horizon, the average computation time per step ranged

between 20 and 30 ms, demonstrating the suitability of the proposed formulation for real-time implementation.

The efficacy of the smoothing method has been demonstrated under three different path scenarios. First scenario shown in Figure 3 that presents a baseline waypoint sequence connected by straight-line segments, highlighting that such a plan, although geometrically correct, is dynamically infeasible for the vessel at service speed; the NMPC-based curvilinear refinement replaces sharp turns with smooth, dynamically compliant arcs, producing corresponding arc-length (ds) and curvature (κ) profiles. In Figure 3a, the initial mission plan comprising four waypoints connected by three straight-line path segments cannot be executed directly due to the vessel's dynamic limitations, particularly at sharp turning points. To ensure feasibility, a nonlinear model predictive control (NMPC) framework based on a curvilinear formulation was applied, explicitly incorporating the vessel's minimum turning radius at its service speed. This process generated the dynamically feasible, smoothed path shown in blue, which replaces the infeasible sharp turns of the original plan. Figure 3b presents the corresponding arc-length increment (ds) and curvature (κ) profiles associated with the smoothed path. It is important to note that these ds and κ profiles represent the reference path geometry to be provided to a vessel's tracking controller. They are not the actual actuator commands. In practice, the real-time tracking controller operating with the vessel's full dynamic model and environmental feedback—would convert these references into actual control inputs, such as rudder angle and engine commands, based on the vessel's measured state and prevailing conditions.

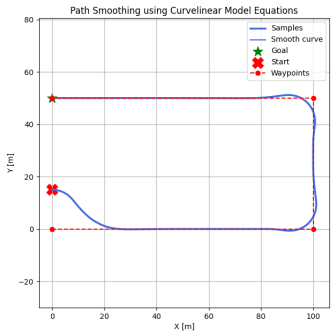

(a) Smoothed Path and Path Segments

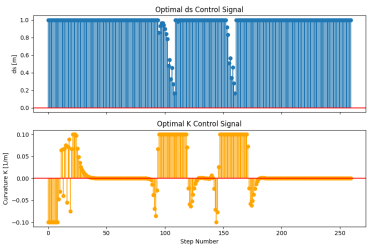

(b) Control signals for ds and K

Figure 3

The second scenario analyzes the impact of κ turn restrictions. Figures 4 and 5 investigate the influence of the minimum turning radius constraint on path geometry within the NMPC-based curvilinear path-following framework, comparing a tighter limit of 10 m (Figures 4a) with a more restrictive 30 m limit (Figures 5a), and showing the resulting changes in curvature demand and path length. In Figure 4, a 10 m turning radius limit allows for tighter curves, enabling the smoothed path (blue) to closely follow the original waypoint layout while remaining dynamically feasible. In contrast, Figure 5 applies a stricter 30 m turning radius constraint, resulting in a noticeably more gradual path that increases the path length but reduces curvature demands. Figures 4a and 5a present the corresponding ds and κ reference profiles. Again, these profiles serve as ref-

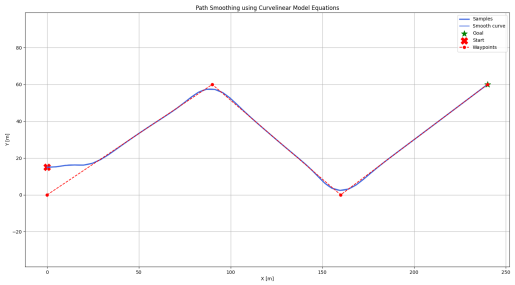

(a) Path Following with NMPC for Curvelinear Model for 10 meters radii

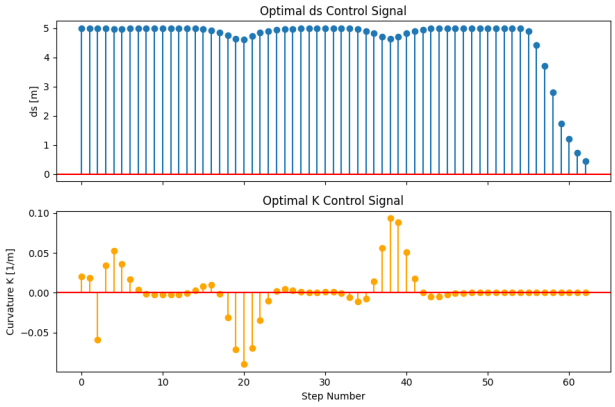

(b) Control signals for ds and K

Figure 4

The last scenario, Figures 6 and 7 demonstrate full integration of the quadtree-based visibility graph with the NMPC smoothing stage in environments containing convex obstacles: the initial collision-free but curvature-agnostic paths (red) are transformed into smooth, feasible trajectories (blue) that maintain safe clearance from obstacles while satisfying turning radius limits, with the associated (κ) and (ds) profiles provided for each scenario. Together, these results confirm the method's ability to adapt to operational constraints, maintain dynamic feasibility, and ensure obstacle avoidance. Figures 6a and 7a present two representative case studies demonstrating the integration of the quadtree-based visibility graph (VG) path planning with the NMPC-based curvilinear smoothing framework in environments containing convex obstacles. In each scenario, the initial path (shown in red) is generated using

the quadtree VG method, ensuring collision-free navigation but without considering the vessel's curvature limitations. To guarantee dynamic feasibility, these preliminary paths are subsequently refined using the curvilinear NMPC formulation, producing the smoothed trajectories shown in blue. This refinement step eliminates sharp turns near obstacles and adjusts the path geometry to respect the vessel's minimum turning radius constraint, while still maintaining a safe clearance from obstacle boundaries. Figures 6b and 7b display the corresponding ds and κ reference histories for these refined paths. These profiles, while useful for visualizing curvature and progression along the path, are again reference geometric signals; the true real-time control inputs (rudder and propulsion commands) would be determined by a lower-level tracking controller. In Scenario 1 (Figures 6a–6b), the planned path includes tighter maneuvers near obstacles, which is reflected in higher curvature peaks and more frequent adjustments in κ. In Scenario 2 (Figures 7a–7b), the environment geometry necessitates longer and more gradual turns, leading to lower curvature magnitudes and smoother ds profiles. Collectively, these results highlight the algorithm's capacity to jointly satisfy collision avoidance, curvature feasibility, and path smoothness, ensuring that the generated reference paths are both safe and dynamically executable by the vessel when tracked by an appropriate real-time control system.

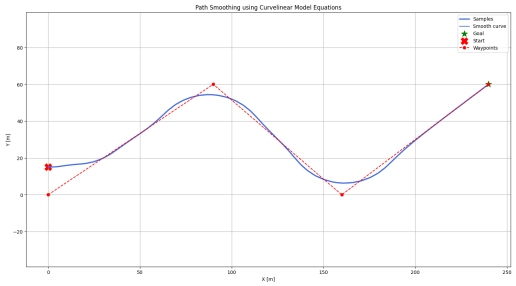

(a) Path Following with NMPC for Curvelinear Model for 30 meters radii

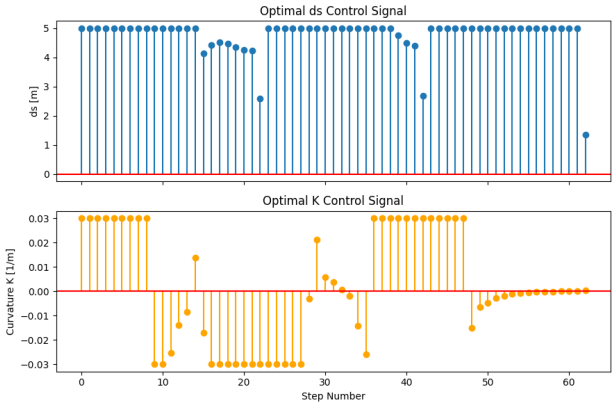

(b) Control signals for ds and K

Figure 5

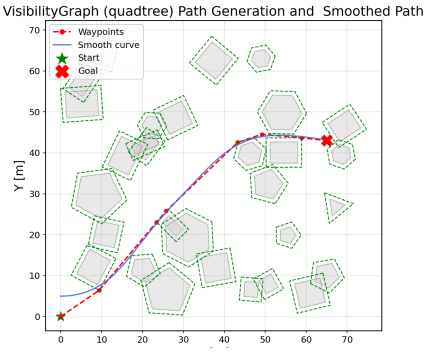

(a) Path Generation and Smoothing Scenario-1

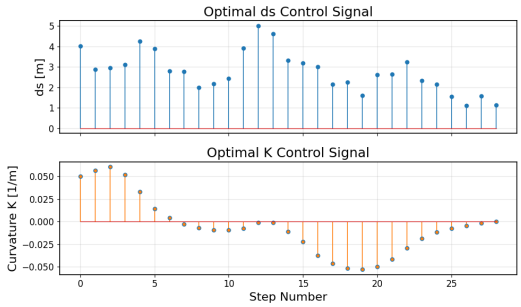

(b) Control signals of ds and K for Path Generation and Smoothing Scenario-1

Figure 6

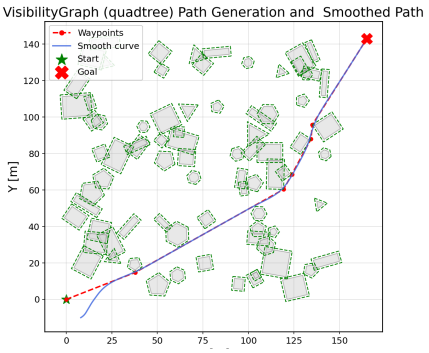

(a) Path Generation and Smoothing Scenario-2

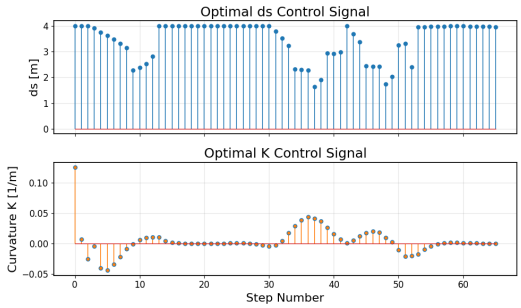

(b) Control signals of ds and K for Path Generation and Smoothing Scenario-2

Figure 7

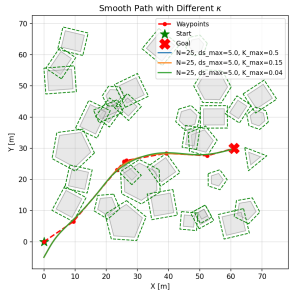

Figure 8: Smoothed path with different κ

Figures 8 illustrates how the paths is smoothed for different curvature values κ. Since κ changes with the vehicle's speed, the figure not only shows the variation of curvature across different velocities but also demonstrates how this variation influences the paths smoothing process. In this way, the method performs smoothing by explicitly considering the vehicle's dynamic motion characteristics that vary with speed.

4 CONCLUSION

This paper introduced a curvature-based kinematic framework for unmanned surface vessel (USV) path planning and motion prediction, formulated in curvilinear coordinates parameterized by curvature κ and arc length s. By integrating empirically derived steady-state turning characteristics, the method captures real vessel maneuvering limits without requiring complex hydrodynamic modeling. The proposed hierarchical architecture combines global path planning via quadtree-based visibility graphs with NMPC-based path refinement, performed as an offline planning stage to generate smooth, collision-free, and dynamically feasible reference trajectories.

Simulation studies demonstrated that the approach produces smooth curvature profiles, reduces control effort, and eliminates sharp turns near obstacles. The ability to adjust minimum turning radius constraints provides adaptability for different vessel types and operational conditions. While the steady-state assumption introduces some conservatism, it enhances computational efficiency and robustness, making the framework suitable for subsequent integration with real-time tracking controllers.

Future work will focus on extending the method to handle dynamic obstacles, incorporating adaptive control for environmental variations, and validating performance through full-scale sea trials. Overall, this study bridges the gap between geometric path planning and vessel dynamics, offering a computationally tractable, physically consistent, and practically implementable solution for autonomous maritime navigation.

REFERENCES

Ravankar, A., Ravankar, A. A., Kobayashi, Y., Hoshino, Y., Peng, C.-C. (2018). 'Path smoothing techniques in robot navigation: State-of-the-art, current and future challenges.' *Sensors*, 18(9), 3170. MDPI.

Mac, T. T., Copot, C., Tran, D. T., De Keyser, R. (2016). 'Heuristic approaches in robot path planning: A survey.' *Robotics and Autonomous Systems*, 86, 13–28. Elsevier.

Sugiura, K., Matsutani, H. (2024). 'An integrated FPGA accelerator for deep learning-based 2D/3D path planning.' *IEEE Transactions on Computers*, 73(6), 1442–1456. IEEE.

Tang, Y., Zakaria, M. A., Younas, M. (2025). 'Path planning trends for autonomous mobile robot navigation: A review.' *Sensors*, 25(4), 1206. MDPI.

Shah, B., Gupta, S. (2016). 'Speeding up A* search on visibility graphs defined over quadtrees to enable long distance path planning for unmanned surface vehicle.' *In Proceedings of the International Conference on Automated Planning and Scheduling*

Lozano-Perez, Tomás; WESLEY, Michael A. (1979). ' An algorithm for planning collision-free paths among polyhedral obstacles.'. *Communications of the ACM*,

Samet, Hanan, and Robert E. Webber. (1985). ' Storing a collection of polygons using quadtrees.'. *ACM Transactions on Graphics (TOG)*,

Hart, Peter E. and Nilsson, Nils J. and Raphael, Bertram.(1968). ' Storing a collection of polygons using quadtrees.'. *ACM Transactions on Graphics (TOG)*,

Allgöwer, Frank, and Alex Zheng(2012). 'Nonlinear model predictive control.'. *ACM Transactions on Graphics (TOG)*,

Allgöwer, Frank, and Alex Zheng(2012). 'Model predictive control: theory, computation, and design. Vol. 2.'. *Madison, WI: Nob Hill Publishing, 2020.*,

Zhu,Man,Xiao,Changshi,Gu,hangding,(2022).'A circle grid-based approach for obstacle avoidance motion planning of unmanned surface vehicles.'*Proceedings of the Institution of Mechanical Engineers, Part M: Journal of Engineering for the Maritime Environment*.

Yang, J., Ni, T., Liu, L., Wen, J., He, J., Li, Z. (2022). 'The Sea Route Planning for Survey Vessel Intelligently Navigating to the Survey Lines.' *Sensors*, 22(2), 482. MDPI.

Wang, X., Jiang, P., Li, D., Sun, T. (2017). 'Curvature continuous and bounded path planning for fixed-wing UAVs.' *Sensors*, 17(9), 2155. MDPI.

Höffmann, M., Patel, S., Büskens, C. (2023). 'Optimal coverage path planning for agricultural vehicles with curvature constraints.' *Agriculture*, 13(11), 2112. MDPI.

Hassani, V., Lande, S. V. (2018). 'Path planning for marine vehicles using Bézier curves.' *IFAC-PapersOnLine*, 51(29), 305–310. Elsevier.

Xu, L., Song, B., Cao, M. (2021). 'A new approach to optimal smooth path planning of mobile robots with continuous-curvature constraint.' *Systems Science & Control Engineering*, 9(1), 138–149. Taylor & Francis.

Scheuer, A., Fraichard, T. (1997). 'Continuous-curvature path planning for car-like vehicles.' *In Proceedings of the 1997 IEEE/RSJ International Conference on Intelligent Robots and Systems (IROS)*, Vol. 2, pp. 997–1003. IEEE.

Heilmeier, A., Wischnewski, A., Hermansdorfer, L., Betz,

J., Lienkamp, M., Lohmann, B. (2020). 'Minimum curvature trajectory planning and control for an autonomous race car.' *Vehicle System Dynamics*. Taylor & Francis.

Rao, A. K., Singh, K. P., Tripathy, T. (2024). 'Curvature bounded trajectories of desired lengths for a Dubins vehicle.' *Automatica*, 167, 111749. Elsevier.

Candeloro, M., Lekkas, A. M., Sørensen, A. J., Fossen, T. I. (2013). 'Continuous curvature path planning using Voronoi diagrams and Fermat's spirals.' *IFAC Proceedings Volumes*, 46(33), 132–137. Elsevier.

Belleter, D. J. W., Paliotta, C., Maggiore, M., Pettersen, K. Y. (2016). 'Path following for underactuated marine vessels.' *IFAC-PapersOnLine*, 49(18), 588–593. Elsevier.

Abrougui, H., Nejim, S., Hachicha, S., Zaoui, C., Dallagi, H. (2021). 'Modeling, parameter identification, guidance and control of an unmanned surface vehicle with experimental results.' *Ocean Engineering*, 241, 110038. Elsevier.

He, Y., Hou, T., Wang, M. (2024). 'A new method for unmanned aerial vehicle path planning in complex environments.' *Scientific Reports*, 14(1), 9257. Nature Publishing Group UK London.

Sinha, S., Farhood, M., Stilwell, D. J. (2025). 'Control design and analysis for autonomous underwater vehicles using integral quadratic constraints.' *Control Engineering Practice*, 154, 106142. Elsevier.

Lobaton, E., Zhang, J., Patil, S., Alterovitz, R. (2011). 'Planning curvature-constrained paths to multiple goals using circle sampling.' *In Proceedings of the 2011 IEEE International Conference on Robotics and Automation*, pp. 1463–1469. IEEE.

Song, C., Guo, T., Sui, J. (2024). 'Ship path planning based on improved multi-scale A* algorithm of collision risk function.' *Scientific Reports*, 14(1), 30418. Nature Publishing Group UK London.

Tam, C., Bucknall, R. (2010). 'Path-planning algorithm for ships in close-range encounters.' *Journal of Marine Science and Technology*, 15(4), 395–407. Springer.

Cui, X., Wang, Y., Yang, S., Liu, H., Mou, C. (2022). 'UAV path planning method for data collection of fixed-point equipment in complex forest environment.' *Frontiers in Neurorobotics*, 16, 1105177. Frontiers Media SA.

Sinha, S., Farhood, M., Stilwell, D. J. (2025). 'Control design and analysis for autonomous underwater vehicles using integral quadratic constraints.' *Control Engineering Practice*, 154, 106142. Elsevier.